

# Numerical simulation on the cavitation of waterjet propulsion pump

C Z Xia, L Cheng<sup>1</sup>, Y N Shang, J R Zhou, F Yang, Y Jin

School of Hydraulic, Energy and power Engineering  
Yangzhou University, Yangzhou, Jiangsu, P.R.China, 225009

E-mail: chengli@yzu.edu.cn

**Abstract.** Waterjet propulsion system is widely used in high speed vessels with advantages of simple transmission mechanism, low noise underwater and good manoeuvrability. Compared with the propeller, waterjet propulsion can be used flow stamping to increasing cavitation resistance at high speed. But under certain conditions, such as low ship speed or high ship speed, cavitation problem still exists. If water-jet propulsion pump is run in cavitation condition for a long time, then the cavitation will cause a great deal of noise CFD is applied to analysis and predict the process of production and development of cavitation in waterjet propulsion pump.

Based on the cavitation model of Zwart-Gerber-Belamri and a mixture of homogeneous flow model, commercial CFD software CFX was taken for characteristics of cavitation under the three operating conditions. Commercial software ANSYS 14.0 is used to build entity model, mesh and numerical simulation. The grid independence analysis determine the grid number of mixed flow pump model is about 1.6 million and the grid number of water-jet pump system unit is about 2.7 million.

The cavitation characteristics of waterjet pump under three operating conditions are studied. The results show that the cavitation development trend is similar design and small rate of flow condition. Under the design conditions Cavitation bubbles are mainly gathered in suction surface of blade near the inlet side of the hub under the primary stage, and gradually extended to the water side in the direction of the rim with the loss of the inlet total pressure. Cavitation appears in hub before the blade rim, but the maximum value of gas content in blade rim is bigger than that in hub. Under large flow conditions, bubble along the direction of wheel hub extends to the rim gradually. Cavitation is found in the pressure surface of blade near the hub region under the critical point of cavitation nearby. When NPSHa is lower than critical point, the area covering by bubbles is about 40% in the suction surface of blade. It means that the critical point of cavitation of pump system is not the accrue point of install cavitation but cavitation has been developed to a certain stage.

## 1. Introduction

Along with the high-speed development of mechanical and military technology, high-speed vessels started to use a new way of special ship propulsion waterjet propulsion. Compared with the traditional propeller, waterjet propulsion system not only has the same good performance in acceleration and braking performance, but also has excellent high speed mobility [1]. The noise and vibration in the

<sup>1</sup> Corresponding author: CHENG Li(1975-), male, PhD, Professor of Yangzhou University



cabin of water jet propulsion ship is small. The waterjet system's daily maintenance is also relatively easy. Waterjet propulsion device in high speed ship can use water to flow stamping improve the cavitation resistance device. But in some special conditions, such as turning, speeding, maneuvering in reverse and only part of the pumps work, the waterjet propulsion system will get into the cavitation workspaces [2]. Cavitation will not only lead to sharp decline in pump hydraulic performance, also can make water jet propulsion pump thrust be reduced, the efficiency decline and reduce the service life of the impeller and bring cavitation, vibration and noise. So the research on water jet propulsion pump system has strong engineering application value and academic significance[3-4].

## 2. Geometric model and numerical method

### 2.1. Geometric model

By changing the propulsion pump in paper [5-6], new propulsion pump is used in this paper which is about the cavitation on the blade of the impeller. In the model, the inlet is extended so that accuracy and convergence for the simulation is solved, the outlet is connected with optimized nozzle. Figure 1 is the computational domains of propulsion pump.

The computational domains contain impeller, vane, inlet and outlet. In which, impeller has six blades and its rotating speed is 700 r/min, vane has seven blades, diameters of inlet and outlet are  $D_0$  and  $1.19D_0$  separately. The straight pipe section shares the same diameter with the inlet. Plane 1 and plane 2 are chosen as the inlet and outlet to calculate the pump head.

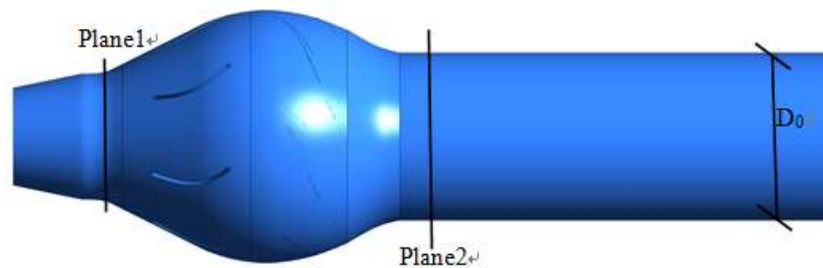
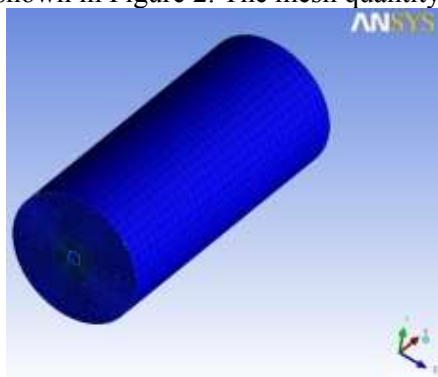


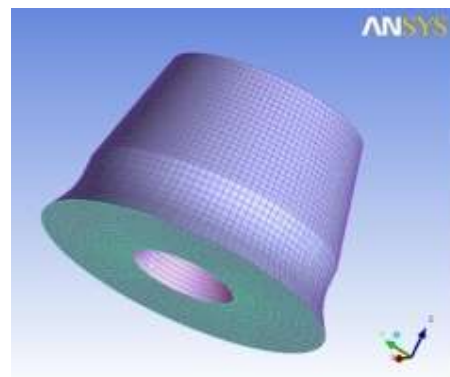
**Figure 1.** Computational domains

### 2.2. Mesh generation

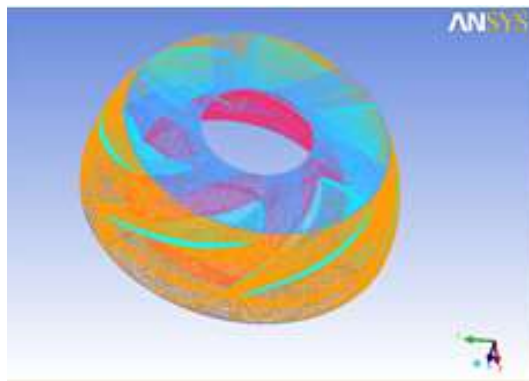
Considering structure mesh accelerating CFD calculation speed, the mesh is generated by using ICEM CFD shown in Figure 2. The mesh quantity is 1.6 million.



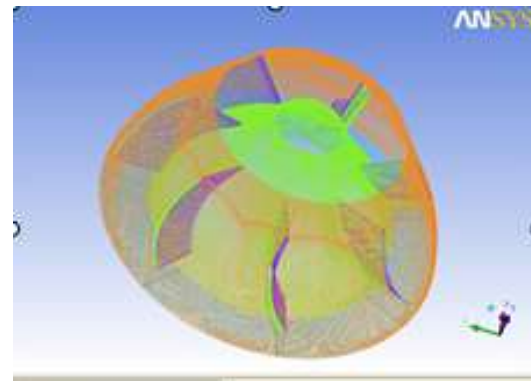
(a) straight pipe section



(b) nozzle



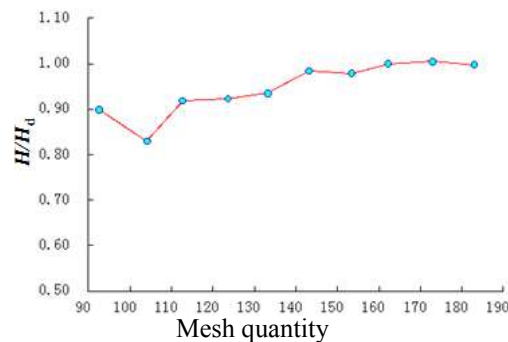
(c) vane



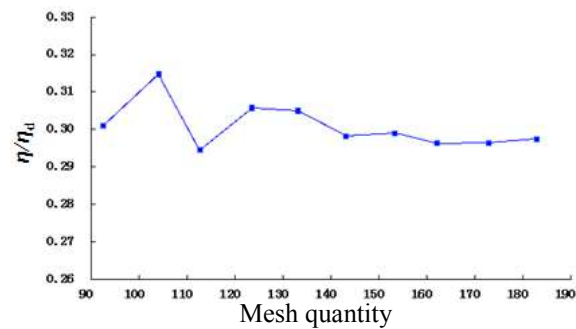
(d) impeller

**Figure 2. Meshes**

In general, mesh quantity affects the accuracy and convergence speed. In theory, more mesh, higher accuracy. Actually, overmuch mesh will increase calculation time and slow convergence speed. The mesh independence discussion is necessary. Impeller is the central domain in the model and its mesh quantity is the key. The result shows that the head and efficiency stay steady when the mesh quantity rises up to 1.6 million.  $H_d$ ,  $\eta_d$  are head and efficiency separately at design condition.



(a) head



(b) efficiency

**Figure 3. Mesh independence**

### 2.3. Boundary condition

Inlet is set as total pressure stable, supposing no cavitation happens in the water. Outlet is set as mass flow rate. When cavitation model is applied, two physical parameters below are given: water's cavitation pressure  $P_v$  equals to 3574Pa at normal atmospheric temperature, cavitation surface tension  $\sigma$  equals to 0.074N/M, Rayleigh—Plesset equation is used to describe bubble motion discipline. No slip wall condition is applied for the wall of hub, rim, blade surface and the other solid walls. The reference pressure is set as 0 atm. RNG  $k-\varepsilon$  model and mixture model are chosen as turbulent model and multiphase flow model separately [6-9].

Calculated result is more close to the test result at large flow rate coefficient by using Zwart-Gerber-Belamri cavitation model, so Zwart-Gerber-Belamri cavitation model [10-14] is chosen to simulate the cavitation in the impeller.

## 3. Results and analysis

Three flow rate conditions are simulated and compared which is design flow rate ( $Q_{bep}$ ), small flow rate ( $0.7 Q_{bep}$ ) and large flow rate ( $1.1 Q_{bep}$ ).

### 3.1. Cavitation performance at design flow rate

Based on the pump performance, the best efficiency point is chosen as the design flow rate which can be down as  $Q_{bep}$ . Different total pressures on the inlet are applied which from 0.5atm to 0.1atm, pressure distributions on the pressure side and suction side of the impeller, cavitation area change is observed.

As shown in Figure 4 and Figure 5, there is pressure distribution on the pressure side and suction side of the impeller separately for different cavitation remainders. In the Figure, the blue area is low pressure zone which firstly appears at the rim of suction side inlet. As NPSHa reduces, low pressure zone increases along blade margin. When NPSHa is 0.76m, the entire suction side of the blade is low pressure zone. Meanwhile, there is also low pressure on the pressure side of blade whose shape is almost triangle, pressure at the hub is larger than it at the rim.

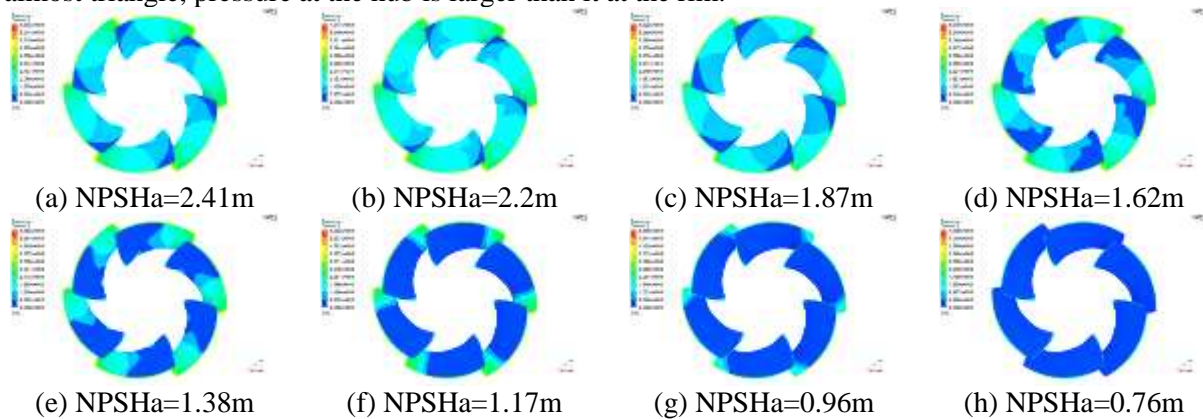


**Figure 4.** Pressure distribution on the suction side of the blade at different cavitation remainders

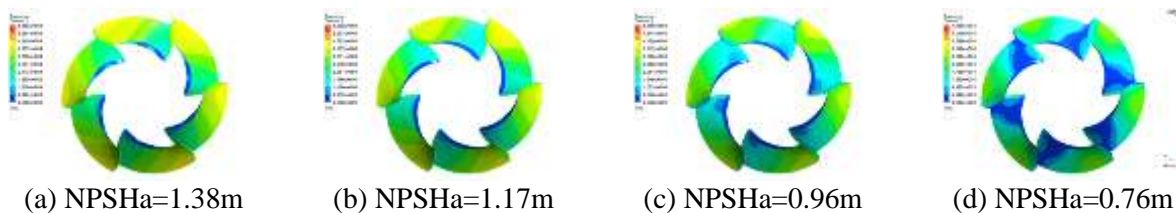


**Figure 5.** Pressure distribution on the pressure side of the blade at different cavitation remainders

Figure 6 and Figure 7 are cavitation volume fraction distribution on the pressure side and suction side of the blade. In the Figure, red zone and blue zone represent large cavitation volume fraction and small cavitation volume fraction. By comparing the pressure distribution on the blade with different cavitation remainders, the same trend is shown. When NPSHa is 0.76m, cavitation on the whole suction pressure has been absolutely developed. The area around the outlet of the blade is affected worst, cavitation will block the entire impeller passage and even result in the cavitation happening on the pressure side of the blade.

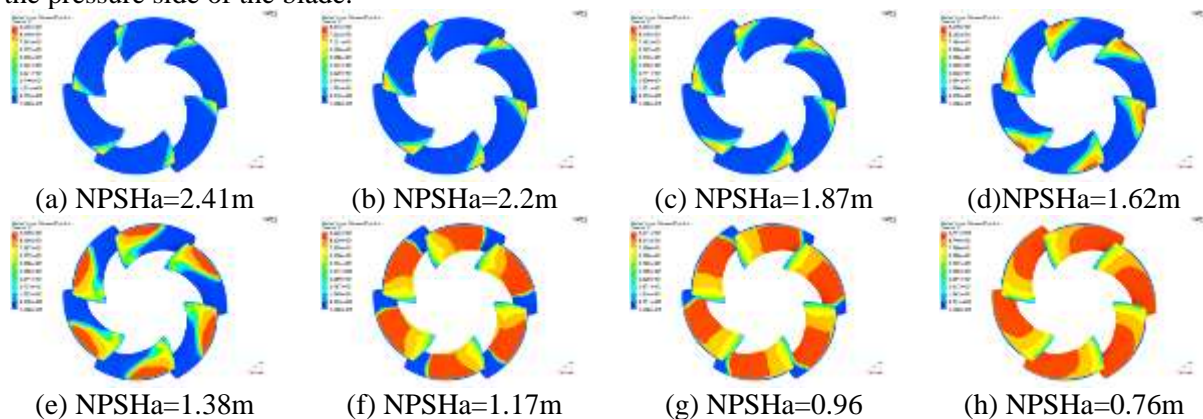


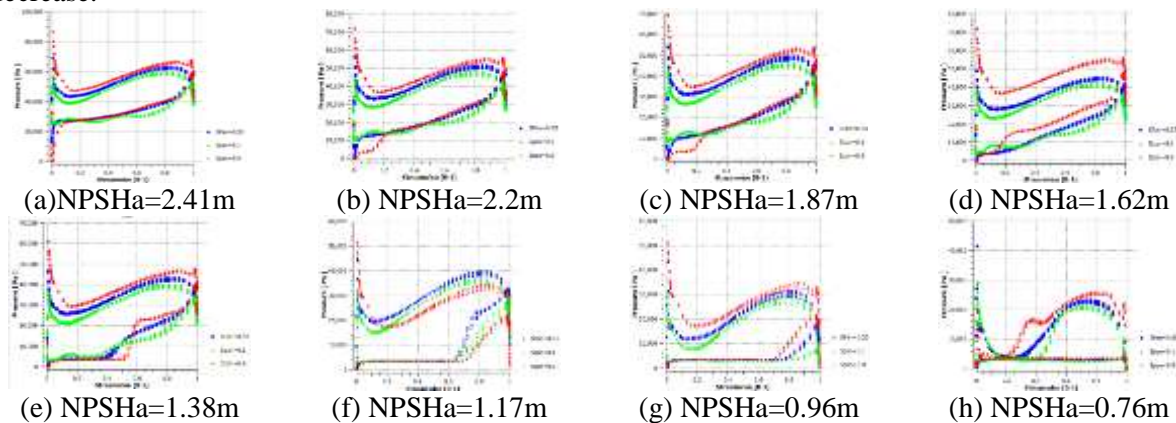
**Figure 6.** Cavitation volume fraction distribution on suction side of the blade





**Figure 7.** Cavitation volume fraction distribution on the pressure side of the blade

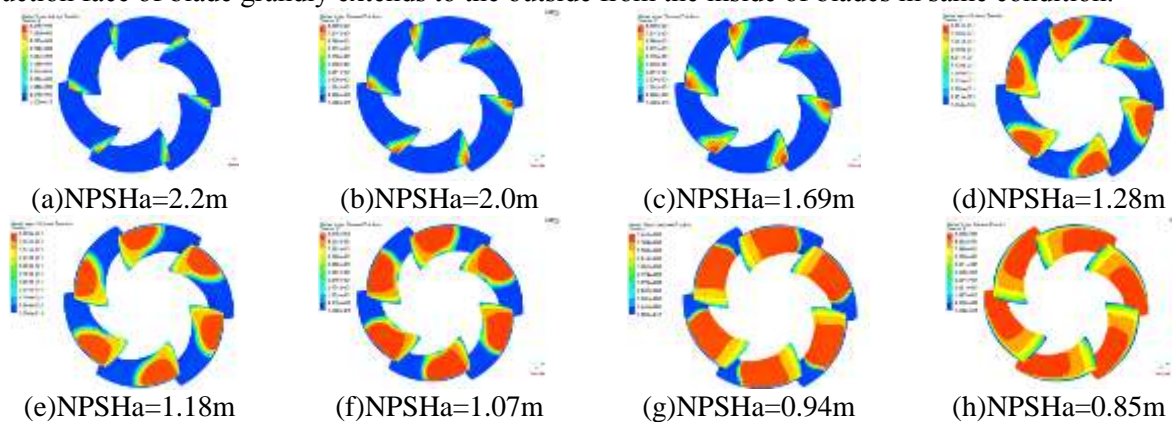
Figure 8 is the static pressure distribution on the blade at different spans. When NPSHa is 2.2m, low static pressure keeps steady. Cavitation happens at the rim of the blade at first. In Figure, on the above and below are the static pressure at the pressure side and suction side respectively. Cavitation will not happen until it happens at the whole suction side. Cavitation at suction side is caused by the low pressure. There is no obvious contact between the cavitation on the pressure side and pressure decrease.



**Figure 8.** Static pressure distribution on the blade at different spans

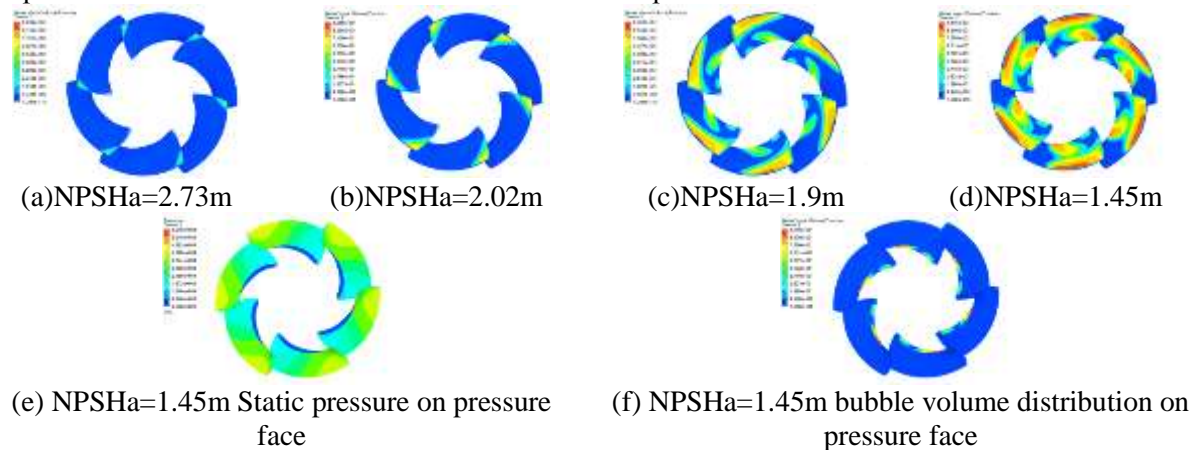
### 3.2. Partial conditions of cavitation characteristics

Figure 9 shows the result of numerical simulation on cavitation in small flow rate. The relation between the distributions of water vapour volume fraction on the suction face of blades and the decreases of NPSHa is show in Figure 9. The result shows that the variations tend of the location of bubble volume fraction distribution are consistent with the design condition. The location of bubble on suction face of blade grandly extends to the outside from the inside of blades in same condition.



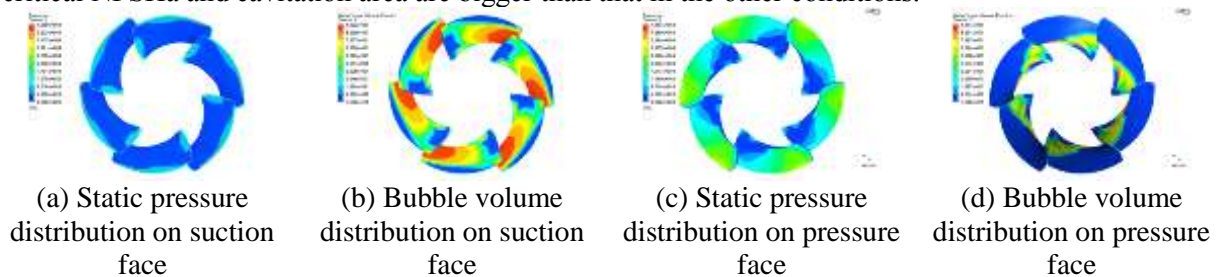
**Figure 9.** the distribution of bubble volume fraction

Figure 10 and Figure 11 show the numerical simulation result of waterjet propulsion pump. The bubbles firstly appear on the edge of the impeller inlet in large flow rate condition, so as in small flow rate and design flow rate. But its variation tendency is greatly different with that in design condition and small flow rate with the decrease of NPSHa. When NPSHa reduces from 1.9m to 1.45m, the region covered by bubble firstly extends along the rim of blade and appears in the middle of blade near the hub. It develops from the hub to the rim of blade. The pressure is higher than the vapour pressure on pressure face of blade. So bubble cannot be found on pressure face of blade.



**Figure 10.** NPSHa>1.45m

While  $NPSHa < 1.45m$ , cavitation is so hard that bubble blocks the passage of impeller. Then the efficiency of pump sharp drop and the pump cannot work. Flow separation is found at the outside edge of suction face of blades for large flow rate and negative angle. Bubble is found on the pressure face and Cavitation volume fraction extends to the rim from the hub at the outside of pressure face. The low pressure area that is blue area showed in Figure 11 is consistent with the distribution of bubble volume fraction. The bubble is found in the large flow rate condition while the development of cavitation is to some extent on the suction face of blade rather than the bubble cover suction face completely in design condition and small flow rate condition. Figure 10 and Figure 11 shows that the critical NPSHa and cavitation area are bigger than that in the other conditions.



**Figure 11.** NPSHa=1.36m

Figure 12 shows the pump cavitation characteristic curve in three working conditions. The flow rate and efficiency curves are showed little change with the decrease of NPSHa. The reason for that is that the flow is unstable in the pump at the begin of bubble produce. But the flow rate and efficiency curves will sharp drop after NPSHa is greater than critical value. The point of critical value is called critical cavitation point. The critical NPSHa decreases as the flow rate reducing and the dropping extent of pump cavitation characteristic curves is small while the flow rate is small. That means that the pump is hard to get cavitation while the flow rate is small.

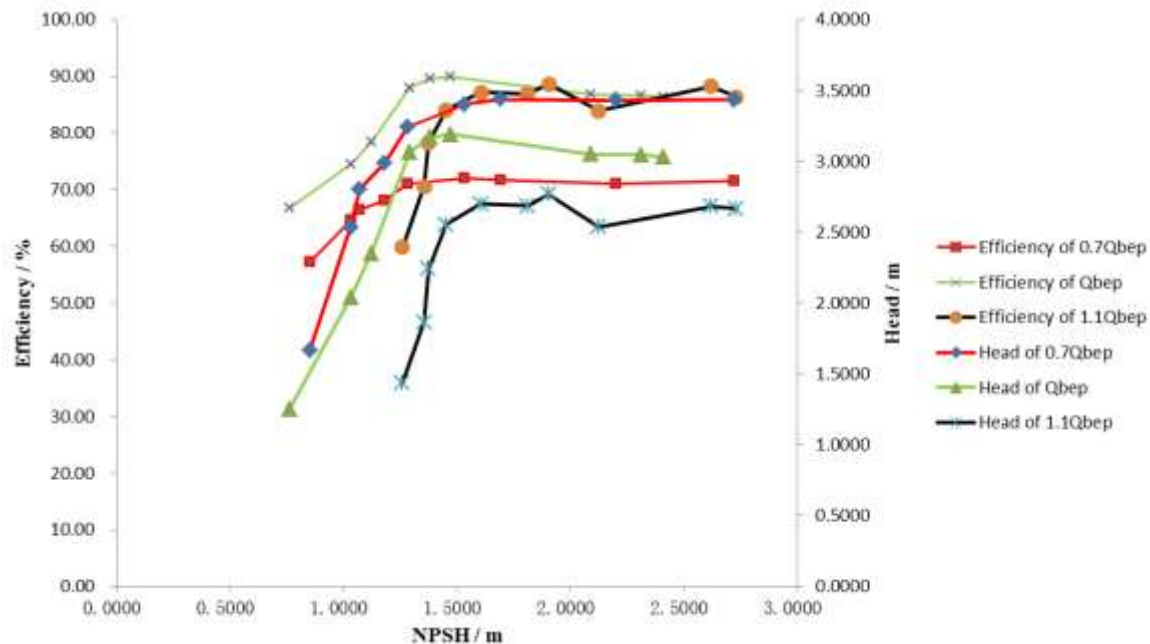


Figure 12 Pump cavitation characteristic curves

#### 4. Conclusions

The paper finds that the cavitation resistances of waterjet propulsion pump are grandly weakened as the critical NPSHa value grandly increase by the numerical simulation on the cavitation flow in waterjet propulsion pump. The harm of cavitation to blades is deepened while deviating from the design operation. The static pressure is bigger in the rim than that in the hub, and the distribution trends of static pressure are almost same in three working condition. Therefore, the bubble volume fraction in the rim is bigger than that in the hub. That means that the cavitation is harder in the rim. And that should be considered in actual design.

#### Acknowledgment

This work was financially supported by National science and technology plan project in rural areas (Grant No.2012BAD08B03), National Natural Science Foundation of China (Grant No. 51179167), Water conservancy science and technology project of Jiangsu Province (Grant No.2014046), The Young academic Leaders in Blue Project of Jiangsu, Prospective Joint Research Project of Jiangsu (Grant No. BY2015061-12), A Project Funded by the Priority Academic Program Development of Jiangsu Higher Education Institutions and Major Natural Science Foundation of Universities in Jiangsu (Grant No.12KJA570001).

#### References

- [1] Wang Y S, Ding J M 2004 Research on the relationship between waterjet power absorption and vessel speed[C]// *International Conference on Waterjet Propulsion*. London: RINA.
- [2] Verbeek R, Bulten N W H 1998 Recent development in waterjet design[C]// *Proceedings of international conference on waterjet propulsion II*. Amsterdam: RINA.
- [3] Harvey E N, Barnes D K, McElroy W D, et al. 1944 Bubble formation in animals. I. Physical factors[J]. *Journal of Cellular and Comparative Physiology*, **24**(1): 1-22.
- [4] Knapp R T, Daily J W, Hammitt F G 1979 *Cavitation*[J].
- [5] Cheng L, Bart P M, Van E, Liu Chao et al. 2012 Radial forces of waterjet propulsion mixed-flow pump[J]. *Journal of Drainage and Irrigation Machinery Engineering*, **30**(6):636-640.

- [6] Bulten N W H, Verbeek R, Van E, Bart P M 2006 CFD simulation of the flow through a waterjet installation[C]//*International Conference on Waterjet Propulsion*. **4**: 11-19.
- [7] Gopalan S, Katz J 2000 Flow structure and modeling issues in the closure region of attached cavitation[J]. *Physics of Fluids(1994-present)*, **12(4)**: 895-911.
- [8] Pham T M, Larrarte F, Fruman D H 1999 Investigation of unsteady sheet cavitation and cloudcavitation mechanisms[J]. *ASME Journal of Fluids Engineering*, **121(2)**: 289-296.
- [9] Pellone C, Peallat J M 1995 Non-linear analysis of three-dimensional partially cavitating hydrofoil[C]//*Proceedings of the International Symposium on Cavitation*, Deauville, France. **1995**: 63-67.
- [10] Yang F, Liu C, Tang F P 2012 Cavitation performance prediction of mixed-flow pump based on CFD[C]//*26th IAHR Symposium on Hydraulic Machinery and System*, August 19-23, 2012, Beijing, China
- [11] Zwart P J, Gerber A G, Belamri T 2004 A two-phase flow model for predicting cavitation dynamics[C]//*Proceedings of the Fifth International Conference on Multiphase Flow*, Yokohama, Japan.
- [12] Orszag S A, Patterson Jr G S 1972 Numerical simulation of three-dimensional homogeneous isotropic turbulence[J]. *Physical Review Letters*, **28(2)**: 76-79.
- [13] Merkle C L, Feng J, Buelow P E O 1998 Computational modeling of the dynamics of sheet cavitation[C]//*Proceedings of Third International Symposium on Cavitation* , Grenoble,France, **1998**:307—311.
- [14] Senocak I , Shyy W 2002 A pressure-based method for turbulent cavitating flow computations[J]. *Journal of Computational Physics*, **176(2)**:363-383.